



Correlative analysis of metabolite profiling of Danggui Buxue Tang in rat biological fluids by rapid resolution LC–TOF/MS

Chang-Yin Li, Lian-Wen Qi*, Ping Li*

Key Laboratory of Modern Chinese Medicines (China Pharmaceutical University), Ministry of Education, Nanjing 210009, China

ARTICLE INFO

Article history:

Received 26 July 2010

Received in revised form

22 December 2010

Accepted 25 December 2010

Available online 13 January 2011

Keywords:

Metabolite profiling

Correlative analysis

Rapid resolution LC–TOF/MS

Danggui Buxue Tang

Plasma

Bile

ABSTRACT

In this work, the metabolite profiles of Danggui Buxue Tang (DBT) in rat bile and plasma were qualitatively described, and the possible metabolic pathways of DBT were subsequently proposed. Emphasis was put on correlative analysis of metabolite profiling in different biological fluids. After oral administration of DBT, bile and plasma samples were collected and pretreated by solid phase extraction. Rapid resolution liquid chromatography coupled to time-of-flight mass spectrometry (RRLC–TOFMS) was used for characterization of DBT-related compounds (parent compounds and metabolites) in biological matrices. A total of 142 metabolites were detected and tentatively identified from the drug-containing bile and plasma samples. Metabolite profiling shows that rat bile contained relatively more glutathione-derived conjugates, more saponins compounds and more diverse forms of metabolites than urine. The metabolite profile in plasma revealed that glucuronide conjugates of isoflavonoids, dimmers, acetylcysteine conjugates and parent form of phthalides, as well as saponin aglycones were the major circulating forms of DBT. Collectively, the metabolite profile analysis of DBT in different biological matrices provided a comprehensive understanding of the *in vivo* metabolic fates of constituents in DBT.

© 2011 Elsevier B.V. All rights reserved.

1. Introduction

Danggui Buxue Tang (DBT), a classical Chinese herbal formula consisting of Radix Astragali and Radix Angelica Sinensis with a weight ratio of 5:1, has been widely used in China since 1247 AD. Traditionally, DBT was prescribed to women in China as a remedy for menopausal symptoms [1]. Nowadays DBT is used not only as an efficacious medicine but also as a common dietary supplement. Modern pharmacological studies have demonstrated that DBT carries various attractive biological activities [2]. The bioactive ingredients of DBT are still not well understood although the chemical constituents of DBT have been systematically studied [3–5].

In the past decade, several *in vitro* methods such as cell extraction [6,7], microdialysis [8], and liposome equilibrium dialysis [9,10] have been applied to screen the bioactive ingredients in DBT. These studies provided helpful information for finally clarifying the therapeutic basis of DBT. However, owing to the inability to conduct comprehensive phase I and II investigations, the artificially high xenobiotic concentration, the lack of gene and protein regulation (such as hormonal regulation) as well as the absence

of sufficient adsorption, distribution, and elimination mechanisms [11], the limitations of such *in vitro* studies are apparent. Considering that *in vivo* metabolism study is closely related to the bioactivity of DBT, it was necessary to perform *in vivo* investigation of DBT metabolism to validate the conclusion from *in vitro* studies and to delineate the complete ADME processes of DBT.

In the past few years, there were several published papers reporting *in vivo* metabolism of DBT [12,13]. In order to get much metabolism information of DBT from the complex biological matrices such as bile, plasma and urine, it is necessary to develop effective and reliable analytical methods for detection. Recently, because of the high speed of analysis, sensitivity and confirmation of structural information, rapid resolution liquid chromatography (RRLC) coupled with time-of-flight mass spectrometry (TOFMS) has become the preferred analytical technique for identifying constituents in Chinese herbal medicines [4,14,15]. As for metabolite identification, TOFMS enables not only the fast detection of data for all expected and unexpected metabolites from a single run, but also reliable and accurate identification for molecular formula and related biotransformation of metabolites [16–18]. Previously, we have developed an RRLC–TOFMS method for characterization of rat urinary metabolite profile of DBT [19], which provided important structural information relating to the metabolism of DBT. As an ongoing work, the aims of this study are to further describe the metabolite profiles of DBT in rat bile and plasma. Highlights will be put on correlative analysis of metabolite profiling in different biological fluids.

* Corresponding authors at: Key Laboratory of Modern Chinese Medicines (China Pharmaceutical University), Ministry of Education, No. 24 Tongjia Lane, Nanjing 210009, China. Tel.: +86 25 83271379; fax: +86 25 83271379.

E-mail addresses: fleude@126.com (L.-W. Qi), liping2004@126.com (P. Li).

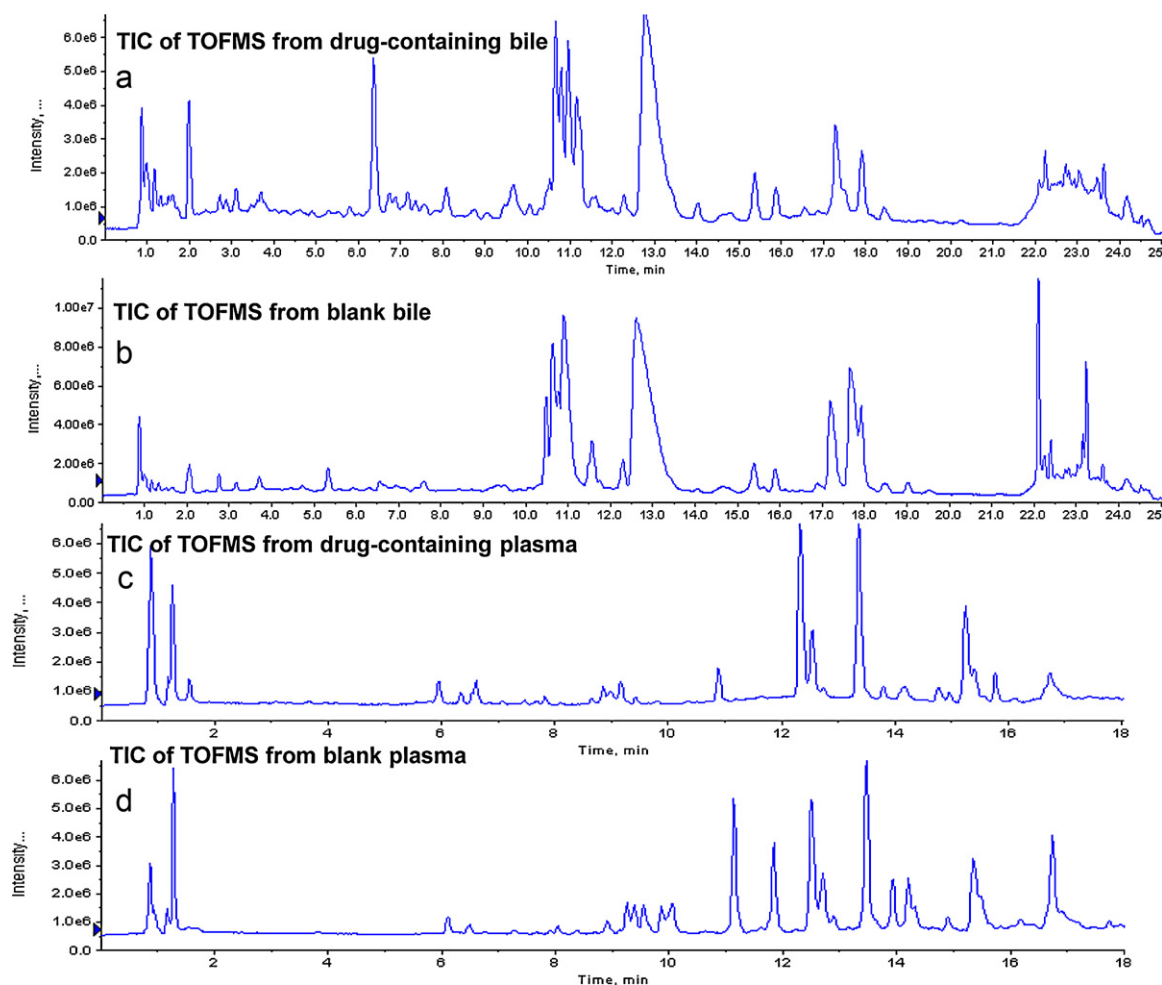


Fig. 1. Total ion chromatograms (TICs) of rat bile and plasma samples in positive ion mode at 120 V fragmentor voltage: (a) the drug-containing bile TIC; (b) the blank bile TIC; (c) the drug-containing plasma TIC; (d) the blank plasma TIC.

2. Experimental

2.1. Materials

The solvents acetonitrile (ACN) and methanol were of HPLC grade from Merck (Darmstadt, Germany). Formic acid with a purity of 96% was purchased from Tedia (Fairfield, OH, USA). Deionized water (18 M Ω) was prepared using the Milli-Q system (Millipore, Milford, MA, USA). Other reagents and chemicals were of analytical grade. DBT oral solution and mixture of authentic standards were prepared by our laboratories as described in the previous study [19].

2.2. Animal protocol

10 male Sprague–Dawley rats (220–250 g) were purchased from Sino-British Sippr/BK Lab Animal Ltd (Shanghai, China). The animals were acclimatized to the facilities for 7 days and then fasted with free access to water for a 12 h period prior to the experiment. The experiments were carried out in accordance with the Guidelines for Animal Experimentation of China Pharmaceutical University (Nanjing, China) and the protocols had been approved by the Animal Ethics Committee of this institution.

Bile sampling: DBT preparation was orally administered to 4 rats at a single dose of approximate 80 g/kg (i.e., 2 mL per 100 g

body weight). The animals were then anesthetized by intraperitoneal injection of 1% pentobarbital sodium (0.15 mL/100 g body weight). An abdominal incision was made and the common bile duct was cannulated with PE-10 tubing (Id = 0.08 cm, Becton Dickinson, USA) for collection of the bile samples. A heating lamp was used for maintaining the body temperatures during the experimental procedures to prevent hypothermic alterations of the bile flow. Drug-containing bile samples were collected for 24 h and stored at -70°C until additional extraction and analysis. Meanwhile, blank bile samples were collected from 2 additional rats.

Plasma collection: Prior to drug administration, blank blood samples were collected from the ophthalmic veins of the rats by sterile capillary tube. Then DBT preparation was orally administered to 4 rats at the dose mentioned above for three consecutive times during a period of 24 h. A volume of 0.8 mL blood sample was collected into heparinized tubes at 1.5 h after the last drug dosing. All blood samples were then centrifuged for 10 min at $4000 \times g$, 4°C , and the supernatants (i.e., the plasma) were stored at -70°C until additional extraction and analysis.

2.3. Sample preparation

In our study, both bile and plasma samples were pretreated with solid phase extraction (SPE) before LC/MS analysis in order to reduce the matrix interference and concentrate the analytes.

Before use, supelclean™ LC-18 SPE columns (1 mL/100 mg volume, Supelco, USA) were conditioned and equilibrated with methanol and deionized water, respectively.

The bile samples (1 mL) were loaded onto the preconditioned SPE columns directly. After washed off with 4 mL of deionized water, the SPE columns were eluted using 2 mL methanol. The eluant was then centrifuged at $14,000 \times g$, 4°C for 10 min, and an aliquot of $1 \mu\text{L}$ supernatants were injected into the RRCL-ESI-TOFMS system for analysis.

After being added $1200 \mu\text{L}$ of methanol, plasma samples ($300 \mu\text{L}$) were vortexed to precipitate plasma proteins, and then centrifuged at $4000 g$, 4°C for 10 min. The supernatants were evaporated to dryness under nitrogen gas at 37°C . The dry residue was reconstituted in 2 mL 95%:5% methanol/water (v/v) solution, fully vortexed, and then loaded onto the preconditioned SPE columns. After washed off with 4 mL of deionized water, the SPE columns were eluted using 2 mL methanol. The eluant was evaporated to dryness in a water bath at 37°C under a nitrogen stream. The residues were reconstituted in $200 \mu\text{L}$ aliquots of HPLC mobile phase, and centrifuged at $14000 g$, 4°C for 10 min. An aliquot of $2 \mu\text{L}$ supernatants were injected into the RRCL-ESI-TOFMS system for analysis.

2.4. Instrumentation and conditions

Chromatographic analysis was performed on an Agilent 1200 Series (Agilent, Germany) rapid resolution LC system equipped with a binary pump, micro degasser, an auto plate-sampler, and a thermostatically controlled column compartment. Chromatographic separation was carried out at 25°C on an Agilent ZorBax SB-C₁₈ column ($4.6 \text{ mm} \times 50 \text{ mm}$, $1.8 \mu\text{m}$). The mobile phase consisted of 0.1% formic acid water (A) and acetonitrile (B), using two different elution gradients for analysis of bile and plasma samples respectively.

The gradient elution for analysis of bile samples was as follows: 0–2 min, 15–21% B; 2–4 min, 21% B; 4–5 min, 21–23% B; 5–8 min, 23% B; 8–9 min, 23–30% B, 9–13 min, 30% B; 13–16 min, 30–37% B; 16–20 min, 37% B; 20–22 min, 37–100% B; 22–25 min, 100% B; 25–27 min, 100–15% B; 27–29 min, 15% B. The flow rate was kept at 0.6 mL/min , and the injecting volume was set at $1 \mu\text{L}$.

The plasma samples were analyzed using a gradient elution of 23% B at 0–3 min, 23–34% B at 3–5 min, 34–40% B at 5–7 min, 40–42% B at 7–8 min, 42–55% B at 8–11.5 min, 55–65% B at 11.5–13 min, 65–75% B at 13–14.5 min, 75–100% B at 14.5–19 min, 100% B at 19–24 min, 100–23% B at 24–26 min, 23% B at 26–28 min. The flow rate was kept at 0.6 mL/min , and the injecting volume was set at $2 \mu\text{L}$.

Detections were performed by an Agilent orthogonal TOF/MS (Agilent Corp, Santa Clara, CA, USA) equipped with ESI source. The TOF/MS analysis worked using full scan mode and mass range was set at m/z 120–2000 in both positive and negative modes. The conditions of ESI source were as follows: drying gas (N_2) flow rate, 9.0 L/min ; drying gas temperature, 325°C ; Nebulizer, 35 psig; capillary voltage, 3000 V; fragmentor voltage, dynamic adjustment from 120 V to 400 V; skimmer voltage, 60 V; OCT RF V, 250 V. The fragmentor voltage was set at 90 V to mainly yield the molecular ion, while 300 V to produce abundant fragment ions. All the operations, acquisition and analysis of data were controlled by Agilent LC-MS/TOF Software Ver. A.01.00 (Agilent Technologies, USA) and Applied Biosystems/MDS-SCIEX Analyst QS Software (Frankfurt, Germany), respectively. Accurate mass measurements (error $<5 \text{ ppm}$) were obtained by an automated calibrant delivery system using a dual-nebulizer ESI source that introduces a low flow ($100 \mu\text{L/min}$) of a calibrating solution (calibrant solution A, Agilent Technologies) [4].

3. Results and discussion

A challenge in metabolic fingerprinting of natural products and herbs is the metabolite identification. Compared with traditional NMR, the coupling of LC and MS has provided an alternative tool for online structural characterization and rapid identification of compounds in complex biological samples. Three types of mass analyzer are commonly used, i.e., quadrupole (Q), ion trap (IT), and time-of-flight (TOF). Quadrupoles are generally used for quantification of target or known compounds. Ion traps have better sensitivity than quadrupoles, and can perform multi-stages of mass spectrometry without additional mass analyzers. TOF/MS analyzers measure mass accurately for the elemental composition of obtained ions and have high resolution and full-scan mass range. More recently, multi-stage MS (also called tandem MS or MS/MS or MSⁿ), combining the different designs of mass analyzers such as triple quadrupole (QqQ), quadrupole ion trap (Q-IT), quadrupole time-of-flight (Q-TOF), and ion trap time-of-flight (IT-TOF), have been emergently introduced. MS/MS with collision-induced dissociation (CID) provides advanced structural information and has better sensitivity, specificity, and versatility. Multi-stage MS, however, is extremely expensive, which makes it unavailable or impractical for most laboratories.

CID can also be achieved in single-stage mass spectrometers (commonly called in-source CID). In this work, one application of in-source CID is achieved in single-stage TOF-MS. The advantage of performing CID in single-stage instruments is simplicity and relatively low cost. The fragmentor in TOF-MS is crucial for efficient transmission of the ions to obtain the best balance between sensitivity and fragmentation.

Fig. 1 shows the typical total ion chromatograms (TICs) of bile and plasma samples in the positive ion mode respectively. By comparing with the blank and drug-containing biological fluids, more endogenous interferences were observed in bile and plasma than in urine [19].

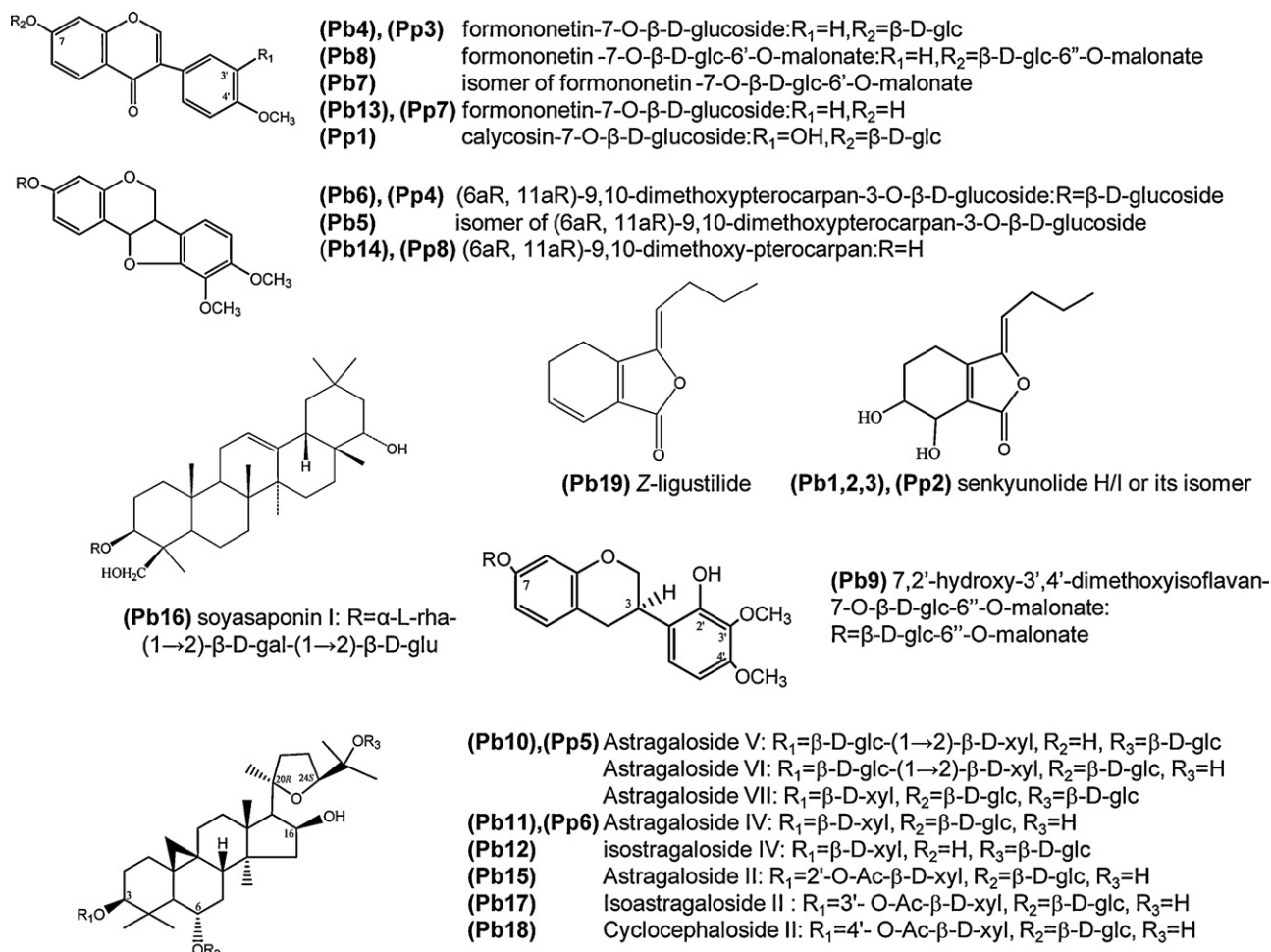
3.1. Detection of parent compounds from biological samples

Endogenous interferences from complex biological matrices usually affect the metabolite identification. To discriminate ions of drug-related peaks from matrix ions from the endogenous interferences, researchers have contributed to development of various techniques for the selective detection of drug metabolites. Since an herb contains complex constituents and many unknown compounds, there is no suitable software available to remove interference ions from drug metabolites in mass spectrometric analyses. To differentiate the drug related peaks from the endogenous interferences, the total ion chromatograms of the drug-containing sample and blank sample were compared to find differences between sample sets. The endogenous interferences can be removed if the accurate retention time and area of the chromatographic peak is identical in the drug-containing and blank samples after creating reconstructed ion chromatograms. Using the extracted ion chromatograms (EICs) of TOFMS, a total of nineteen and eight parent compounds were detected from the drug-containing bile and plasma samples, respectively. Table 1 summarizes the accurate mass measurements for the protonated molecules of the parent constituents in positive ion mode. Retention times, formulas, experimental and theoretical masses, mDa and ppm errors, and double-bond equivalent index (DBE) are included. Since the structural characterization of constituents in DBT has been well elucidated in our previous work [4], these parent compounds can be identified according to calculated formula, obtained diagnostic ions and fragmentation information. Most of the parent compounds were further confirmed by comparison of their retention times and TOFMS data with

Table 1

Accurate mass measurement for the protonated molecules of parent compounds in rat bile and plasma.

No.	t_R (min)	Experimental m/z	Formula	Calculated m/z	mDa error	ppm error	DBE
Parent compounds in rat bile (Pb)							
Pb1 ^a	6.964	225.1111	C ₁₂ H ₁₇ O ₄	225.1121	-1.0	-4.6	4.5
Pb2	7.923	225.1131	C ₁₂ H ₁₇ O ₄	225.1121	1.0	4.3	4.5
Pb3	9.008	225.1116	C ₁₂ H ₁₇ O ₄	225.1121	-0.5	-2.4	4.5
Pb4 ^a	9.246	431.1330	C ₂₂ H ₂₃ O ₉	431.1336	-0.7	-1.5	11.5
Pb5	10.278	463.1621	C ₂₃ H ₂₇ O ₁₀	463.1598	2.2	4.8	10.5
Pb6 ^a	10.875	463.1592	C ₂₃ H ₂₇ O ₁₀	463.1598	-0.7	-1.5	10.5
Pb7	11.397	517.1333	C ₂₅ H ₂₅ O ₁₂	517.1340	-0.8	-1.5	13.5
Pb8	11.885	517.1349	C ₂₅ H ₂₅ O ₁₂	517.1340	0.8	1.6	13.5
Pb9	13.495	551.1732	C ₂₆ H ₃₁ O ₁₃	551.1759	-2.7	-4.9	11.5
Pb10	13.658	947.5196	C ₄₇ H ₇₉ O ₁₉	947.5210	-1.4	-1.5	8.5
Pb11 ^a	15.468	785.4617	C ₄₁ H ₆₉ O ₁₄	785.4681	-6.5	-8.3	7.5
Pb12	17.693	785.4660	C ₄₁ H ₆₉ O ₁₄	785.4681	-2.2	-2.8	7.5
Pb13 ^a	18.345	269.0797	C ₁₆ H ₁₃ O ₄	269.0808	-1.1	-4.2	10.5
Pb14 ^a	19.267	301.1068	C ₁₇ H ₁₇ O ₅	301.1070	-0.3	-0.8	9.5
Pb15	20.208	827.4718	C ₄₃ H ₇₁ O ₁₅	827.4787	-6.9	-8.4	8.5
Pb16	21.891	943.5257	C ₄₈ H ₇₉ O ₁₈	943.5260	-0.4	-0.4	9.5
Pb17	21.927	827.4814	C ₄₃ H ₇₁ O ₁₅	827.4787	2.7	3.2	8.5
Pb18	22.126	827.4787	C ₄₃ H ₇₁ O ₁₅	827.4787	0.0	-0.1	8.5
Pb19 ^a	23.085	191.1062	C ₁₂ H ₁₅ O ₂	191.1066	-0.5	-2.4	5.5
Parent compounds in rat plasma (Pp)							
Pp1 ^a	2.017	447.1277	C ₂₂ H ₂₃ O ₁₀	447.1285	-0.9	-2.0	11.5
Pp2 ^a	5.473	225.1134	C ₁₂ H ₁₇ O ₄	225.1121	1.3	5.6	4.5
Pp3 ^a	5.744	431.1352	C ₂₂ H ₂₃ O ₉	431.1336	1.5	3.6	11.5
Pp4 ^a	6.432	463.1595	C ₂₃ H ₂₇ O ₁₀	463.1598	-0.4	-0.8	10.5
Pp5	7.047	947.519	C ₄₇ H ₇₉ O ₁₉	947.5210	-2.0	-2.1	8.5
Pp6 ^a	8.494	807.4421	C ₄₁ H ₆₈ O ₁₄ Na	807.4501	-8.0	-9.9	7.5
Pp7 ^a	9.888	269.0786	C ₁₆ H ₁₃ O ₄	269.0808	-2.2	-8.3	10.5
Pp8 ^a	10.376	301.106	C ₁₇ H ₁₇ O ₅	301.1070	-1.1	-3.5	9.5

^a Further confirmation in comparison with reference compounds.**Fig. 2.** Chemical structures of parent compounds in rat bile (Pb) and plasma (Pp) samples.

those of reference compounds. Their structures are shown in Fig. 2.

3.2. Characterization of DBT-related metabolites in bile and plasma

The strategies for metabolite detection and identification were similar with the previous study [19]. Briefly, DBT-related metabolites were screened from the drug-containing biological matrix by comparing the TIC data with those from blank biological samples. The molecular ions of metabolites was then determined based on $[M+H]^+/[M+Na]^+/[M+NH_4]^+$ in positive mode and $[M-H]^-$ in negative ion mode using a gentle 120 V fragmentor. The accurate molecular formula of each metabolite was calculated with different criteria including acceptable accuracy threshold, the number of nitrogen atoms, the DBE index, and 'show isotopic' function [20]. Using a high 300 V fragmentor, fragment ions were recorded for the metabolites. MS data of metabolites were then correlated with those of original constituents in DBT. Possible metabolites were finally predicted and potential metabolic pathways were enclosed. Using this strategy, totally one hundred and forty two metabolites were detected in drug-containing bile and plasma samples, respectively. Tables 2 and 3 summarize the accurate mass measurements information including the retention times, formulas, experimental and theoretical masses, mDa and ppm errors, and DBE for the protonated molecules of metabolites in rat bile and plasma. The exact identification of each group of components is outlined below. Of note, the disadvantage of CID in single-stage TOF/MS is that a specific precursor ion cannot be selected so the source of product ions cannot be determined. This seems to particularly be difficult for prediction of overlapped peaks. In this work, we used a RRLC to obtain high resolution in metabolite separation and tried to make all peaks be achieved base-line separation.

3.2.1. Characterization of biliary metabolites

As can be seen from Fig. 1, the endogenous compounds and targets were present in higher concentration in bile than in plasma and in urine. Our preliminary experiments showed that smaller injection volume offered better sensitivity for metabolites in bile. As a result, we used 2 mL MeOH collection and 1 μ L injection volume for bile sample instead of 200 μ L MeOH collection and 1 μ L injection volume for blood sample. As shown in Table 2, up to one hundred DBT-related metabolites were detected from the drug-containing bile sample. Comparing with urinary metabolites [19], there were forty five common metabolites detected both in bile and urine. All metabolites except for B50, B58, B81, B86 and B92 were tentatively identified. They are assigned into three groups: isoflavonoid-related, phthalide-related and saponin-related metabolites, shown in Tables 4–6, respectively.

3.2.1.1. Isoflavonoid-related metabolites. Chemical investigations revealed that isoflavonoids in DBT preparation possessed four major types of aglycone, i.e., calycosin, formononetin, 9,10-dimethoxypterocarpan (DMP) and 7,2'-hydroxy-3',4'-dimethoxyisoflavan (HDMF) [4]. According to the correlation with the four parent aglycones, the structures and origins of the isoflavonoid metabolites can be tentatively deduced. A total of fifty metabolites were assigned as metabolites of isoflavonoids, including 21 common metabolites also detected in urine. Among these, B13, B62 and B49 were firstly detected in this work. As shown in Fig. 3, B13 and B62 yielded the same characterized ions including $[M+H]^+$ at m/z 451.126 ($C_{21}H_{23}O_{11}$) and the aglycone ion $[M-C_6H_8O_6+H]^+$ at m/z 275.09 ($C_{15}H_{15}O_5$) at the fragmentor voltage of 120 V in the positive ion mode, indicating that they were isomers of glucuronide conjugates. The relations of elemental compositions between the aglycone ($C_{15}H_{14}O_5$) and four parent

aglycones (calycosin ($C_{16}H_{12}O_5$), formononetin ($C_{16}H_{12}O_4$), DMP ($C_{17}H_{18}O_5$) and HDMF ($C_{17}H_{18}O_5$)) suggested that demethylation was an essential step for the formation of this aglycone, while hydrogenation and hydroxylation may be also involved. With the same molecular formula and similar mass spectrum (data not shown), B49 as well as 9 biliary metabolites (only present in bile), i.e., B7, B10, B20, B23, B25, B30, B36, B43 and B53, were considered as isomers of the 21 identified metabolites. The possible structures of B27 and B28, two unidentified metabolites in the previous study [19], were also characterized in this work.

Besides, there were still 17 unique isoflavonoids metabolites in the drug-containing bile. Table 4 summarized the diagnostic molecular ions, fragment ions and possible origin of each metabolite, and major metabolic pathways involved. Based on the presence of diagnostic loss of $C_6H_8O_6$, all the metabolites except for B3, were assigned as glucuronide conjugates. The aglycone ($C_{16}H_{14}O_5$) of B41 and B46 was formed via hydrogenation of calycosin ($C_{16}H_{12}O_5$) at the C2–3 double bond of C-ring [21]. The glucuronide conjugation positions of B41 and B46 were assigned to be C7 and C3' respectively due to their differences in peak abundance [22,23]. For the largest group isomers including B11, B16, B29, B32, B37 and B45, the DBE value suggested that the aglycone possessed an isoflavan skeleton, which may be generated via demethylation and hydrogenation of calycosin or formononetin. Alternatively, the aglycone may also be formed from HDMF via demethylation and deoxygenation. Elemental composition correlation revealed that the aglycone ($C_{17}H_{18}O_6$) of B15, B22 and B24 can be generated via hydration of DMP ($C_{17}H_{16}O_5$) or hydroxylation of HDMF ($C_{17}H_{18}O_5$), while the aglycone ($C_{16}H_{14}O_3$) of B51 and B83 was deduced as metabolites of formononetin ($C_{16}H_{12}O_4$). The aglycone of B65 has the chemical formula of $C_{17}H_{14}O_5$, 2 H less than $C_{17}H_{16}O_5$, suggesting that it may be formed by dehydrogenation of DMP. According to the metabolism studies of isoflavonoids [21,24,25], the aglycone of B38 may be generated from calycosin or formononetin via hydroxylation and methylation. The aglycone ion was not found in the mass spectrum of B14. This metabolite can be tentatively assigned as a glucuronide conjugate of isoflavanone, which was probably generated by hydrogenation and glucuronidation of formononetin. B3 is a special metabolite showing the diagnostic loss of $C_6H_{10}O_5$. According to basic metabolism rules and the presence of the aglycone ion 301.0723 ($C_{16}H_{13}O_6$), B3 may be generated from calycosin-7-O- β -D-glucoside via hydroxylation, or from formononetin-7-O- β -D-glucoside via dihydroxylation. However, the position of hydroxylation cannot be determined.

As discussed above, it was common that several metabolites were assigned as isomers in biological matrices according to the same molecular formula. Correspondingly, in some cases, different alternative structures were possible for an observed biotransformation. Elucidation and discrimination of the exact structure of each isomer, such as position of hydroxylation or conjugation, was beyond the capacity of the current analytical instrumentation. Fig. 4 summarizes possible structures of all isoflavonoids metabolites in bile and metabolic pathways involved in their formation.

3.2.1.2. Phthalide-related metabolites. A total of forty metabolites were characterized as phthalides-related metabolites in the drug-containing bile. Seventeen of them were also detected in rat urine, including two new metabolites B4 and B77 which were considered as isomers of B5 and B78 respectively. Moreover, five unique biliary metabolites, B18, B26, B39, B66 and B88, were assigned as isomers of these common metabolites. Table 5 summarized the data for characterization of other eighteen unique phthalide-related metabolites, including the possible origins and metabolic pathways. Among them, B61, B89, B94 and B96 were assigned as isomers of butylidenephthalide-related metabolites, which may be formed via sequential hydration and methylation of butylidenephthalide.

Table 2
Accurate mass measurement for the protonated molecules of metabolites in rat bile (B).

No.	t_R (min)	Experimental m/z	Formula	Calculated m/z	mDa error	ppm error	DBE
B1 ^a	2.694	623.1598	C ₂₈ H ₃₁ O ₁₆	623.1606	-0.9	-1.4	13.5
B2 ^a	2.784	305.1256	C ₁₃ H ₂₁ O ₈	305.1230	2.5	8.2	3.5
B3	3.254	463.1252	C ₂₂ H ₂₃ O ₁₁	463.1234	1.7	3.7	11.5
B4 ^a	3.254	386.1275	C ₁₇ H ₂₄ NO ₇ S	386.1268	0.7	1.8	6.5
B5 ^a	3.435	386.1276	C ₁₇ H ₂₄ NO ₇ S	386.1268	0.8	2.1	6.5
B6 ^a	3.472	431.0988	C ₂₁ H ₁₉ O ₁₀	431.0972	1.5	3.5	12.5
B7 ⁺	3.653	461.1086	C ₂₂ H ₂₁ O ₁₁	461.1078	0.8	1.7	12.5
B8 ^a	3.689	465.139	C ₂₂ H ₂₅ O ₁₁	465.1391	-0.1	-0.3	10.5
B9 ^a	3.707	386.126	C ₁₇ H ₂₄ NO ₇ S	386.1268	-0.8	-2.1	6.5
B10 ⁺	3.725	461.1076	C ₂₂ H ₂₁ O ₁₁	461.1078	-0.2	-0.5	12.5
B11	4.069	452.1558	C ₂₁ H ₂₆ NO ₁₀	452.1551	0.7	1.5	9.5
B12 ^a	4.250	493.1331	C ₂₃ H ₂₅ O ₁₂	493.1340	-1.0	-1.9	11.5
B13 ^a	4.286	451.1256	C ₂₁ H ₂₃ O ₁₁	451.1234	2.1	4.7	10.5
B14	4.503	447.1277	C ₂₂ H ₂₃ O ₁₀	447.1285	-0.9	-2.0	11.5
B15	4.575	495.1482	C ₂₃ H ₂₇ O ₁₂	495.1497	-1.5	-3.0	10.5
B16	4.720	435.128	C ₂₁ H ₂₃ O ₁₀	435.1285	-0.6	-1.3	10.5
B17	4.901	368.1164	C ₁₇ H ₂₂ NO ₆ S	368.1162	0.2	0.4	7.5
B18	4.937	400.1616	C ₁₈ H ₂₆ NO ₉	400.1602	1.4	3.5	6.5
B19	4.937	447.0937	C ₂₁ H ₁₉ O ₁₁	447.0921	1.5	3.4	12.5
B20 ⁺	5.010	477.1413	C ₂₃ H ₂₅ O ₁₁	477.1391	2.2	4.5	11.5
B21	5.191	368.1146	C ₁₇ H ₂₂ NO ₆ S	368.1162	-1.6	-4.4	7.5
B22	5.353	495.1509	C ₂₃ H ₂₇ O ₁₂	495.1497	1.2	2.4	10.5
B23 ^a	5.480	447.0924	C ₂₁ H ₁₉ O ₁₁	447.0921	0.2	0.5	12.5
B24	5.570	495.1516	C ₂₃ H ₂₇ O ₁₂	495.1497	1.9	3.8	10.5
B25 ^a	5.607	465.1366	C ₂₂ H ₂₅ O ₁₁	465.1391	-2.5	-5.5	10.5
B26	5.788	402.1742	C ₁₈ H ₂₈ NO ₉	402.1758	-1.7	-4.1	5.5
B27 ^a	5.806	479.1919	C ₂₄ H ₃₁ O ₁₀	479.1911	0.7	1.5	9.5
B28 ^a	5.824	399.0753	C ₁₇ H ₁₉ O ₉ S	399.0744	0.9	2.2	8.5
B29	5.878	435.129	C ₂₁ H ₂₃ O ₁₀	435.1285	0.4	1.0	10.5
B30 ⁺	6.023	477.1046	C ₂₂ H ₂₁ O ₁₂	477.1027	1.8	3.9	12.5
B31	6.186	465.1398	C ₂₂ H ₂₅ O ₁₁	465.1391	0.7	1.4	10.5
B32	6.204	435.1301	C ₂₁ H ₂₃ O ₁₀	435.1285	1.5	3.5	10.5
B33 ^a	6.204	365.0335	C ₁₆ H ₁₃ O ₈ S	365.0325	0.9	2.6	10.5
B34 ^a	6.330	401.1448	C ₁₈ H ₂₅ O ₁₀	401.1442	0.6	1.4	6.5
B35 ^a	6.367	461.1089	C ₂₂ H ₂₁ O ₁₁	461.1078	1.1	2.3	12.5
B36 ⁺	6.475	479.1534	C ₂₃ H ₂₇ O ₁₁	479.1547	-1.4	-2.9	10.5
B37	6.692	435.1263	C ₂₁ H ₂₃ O ₁₀	435.1285	-2.3	-5.2	10.5
B38	6.819	491.1185	C ₂₃ H ₂₃ O ₁₂	491.1184	0.1	0.2	12.5
B39	6.964	402.1765	C ₁₈ H ₂₈ NO ₉	402.1758	0.6	1.6	5.5
B40	6.982	387.1648	C ₁₈ H ₂₇ O ₉	387.1649	-0.2	-0.4	5.5
B41	7.054	463.1245	C ₂₂ H ₂₃ O ₁₁	463.1234	1.0	2.2	11.5
B42 ^a	7.054	477.1036	C ₂₂ H ₂₁ O ₁₂	477.1027	0.8	1.8	12.5
B43 ⁺	7.108	465.1376	C ₂₂ H ₂₅ O ₁₁	465.1391	-1.5	-3.3	10.5
B44	7.163	385.1429	C ₁₇ H ₂₅ N ₂ O ₆ S	385.1427	0.1	0.3	6.5
B45	7.253	435.1289	C ₂₁ H ₂₃ O ₁₀	435.1285	0.3	0.7	10.5
B46	7.326	463.1246	C ₂₂ H ₂₃ O ₁₁	463.1234	1.1	2.4	11.5
B47	7.344	514.1842	C ₂₂ H ₃₂ N ₃ O ₉ S	514.1853	-1.2	-2.3	8.5
B48	7.525	385.142	C ₁₇ H ₂₅ N ₂ O ₆ S	385.1427	-0.8	-2.0	6.5
B49 ^a	7.597	493.1342	C ₂₃ H ₂₅ O ₁₂	493.1340	0.1	0.3	11.5
B50 ^a	7.615	371.1322	C ₁₇ H ₂₃ O ₉	371.1336	-1.5	-3.9	6.5
B51	7.778	431.1369	C ₂₂ H ₂₃ O ₉	431.1336	3.2	7.5	11.5
B52 ^a	7.778	381.1173	C ₁₈ H ₂₁ O ₉	381.1180	-0.7	-1.9	8.5
B53 ⁺	8.010	493.1339	C ₂₃ H ₂₅ O ₁₂	493.1340	-0.2	-0.3	11.5
B54	8.086	514.1863	C ₂₂ H ₃₂ N ₃ O ₉ S	514.1853	0.9	1.8	8.5
B55	8.375	387.1647	C ₁₈ H ₂₇ O ₉	387.1649	-0.3	-0.7	5.5
B56	8.628	385.1424	C ₁₇ H ₂₅ N ₂ O ₆ S	385.1427	-0.4	-1.0	6.5
B57 ^a	8.755	400.1595	C ₁₈ H ₂₆ NO ₉	400.1602	-0.7	-1.8	6.5
B58 ^a	8.809	371.1335	C ₁₇ H ₂₃ O ₉	371.1336	-0.2	-0.4	6.5
B59 ^a	8.900	285.0417	C ₁₂ H ₁₃ O ₆ S	285.0427	-1.0	-3.6	6.5
B60 ^a	9.026	419.1328	C ₂₁ H ₂₃ O ₉	419.1336	-0.9	-2.0	10.5
B61	9.099	221.1167	C ₁₃ H ₁₇ O ₃	221.1172	-0.5	-2.4	5.5
B62 ^a	9.461	451.1226	C ₂₁ H ₂₃ O ₁₁	451.1234	-0.9	-2.0	10.5
B63 ^a	9.660	445.1132	C ₂₂ H ₂₁ O ₁₀	445.1129	0.3	0.6	12.5
B64 ^a	9.967	477.1031	C ₂₂ H ₂₁ O ₁₂	477.1027	0.3	0.7	12.5
B65	10.040	475.1258	C ₂₃ H ₂₃ O ₁₁	475.1234	2.3	4.9	12.5
B66	10.601	405.1157	C ₁₈ H ₂₂ O ₉ Na	405.1156	0.1	0.2	7.5
B67 ^a	10.619	465.1373	C ₂₂ H ₂₅ O ₁₁	465.1391	-1.8	-4.0	10.5
B68 ^a	10.800	402.1764	C ₁₈ H ₂₈ NO ₉	402.1758	0.5	1.3	5.5
B69	10.818	397.1124	C ₁₈ H ₂₁ O ₁₀	397.1129	-0.5	-1.3	8.5
B70 ^a	10.872	509.163	C ₂₄ H ₂₉ O ₁₂	509.1653	-2.4	-4.6	10.5
B71 ^a	10.999	465.1378	C ₂₂ H ₂₅ O ₁₁	465.1391	-1.3	-2.9	10.5
B72 ^a	11.161	477.1379	C ₂₃ H ₂₅ O ₁₁	477.1391	-1.2	-2.6	11.5
B73 ^a	11.252	479.1545	C ₂₃ H ₂₇ O ₁₁	479.1547	-0.3	-0.6	10.5
B74	11.306	404.19	C ₁₈ H ₃₀ NO ₉	404.1915	-1.5	-3.7	4.5

Table 2 (Continued)

No.	t_R (min)	Experimental m/z	Formula	Calculated m/z	mDa error	ppm error	DBE
B75 ^a	11.722	479.1535	C ₂₃ H ₂₇ O ₁₁	479.1547	-1.3	-2.7	10.5
B76 ^a	11.759	349.0365	C ₁₆ H ₁₃ O ₇ S	349.0376	-1.2	-3.3	10.5
B77 ^a	11.976	370.131	C ₁₇ H ₂₄ NO ₆ S	370.1318	-0.9	-2.4	6.5
B78 ^a	12.681	370.131	C ₁₇ H ₂₄ NO ₆ S	370.1318	-0.9	-2.4	6.5
B79 ^a	12.916	352.1225	C ₁₇ H ₂₂ NO ₅ S	352.1213	1.2	3.3	7.5
B80 ^a	12.935	259.1644	C ₁₂ H ₂₃ N ₂ O ₄	259.1652	-0.8	-3.2	2.5
B81 ^a	13.387	354.1363	C ₁₇ H ₂₄ NO ₅ S	354.1369	-0.7	-1.9	6.5
B82 ^a	13.459	352.1215	C ₁₇ H ₂₂ NO ₅ S	352.1213	0.2	0.5	7.5
B83	14.545	431.1371	C ₂₂ H ₂₃ O ₉	431.1336	3.4	8.0	11.5
B84 ^a	17.476	352.1207	C ₁₇ H ₂₂ NO ₅ S	352.1213	-0.6	-1.8	7.5
B85 ^a	19.593	292.1013	C ₁₅ H ₁₈ NO ₃ S	292.1001	1.1	3.8	7.5
B86	19.883	675.4051	C ₃₆ H ₆₀ O ₁₀ Na	675.4078	-2.8	-4.1	6.5
B87	20.281	645.3949	C ₃₅ H ₅₈ O ₉ Na	645.3973	-2.4	-3.7	6.5
B88	21.203	399.2161	C ₂₄ H ₃₁ O ₅	399.2166	-0.5	-1.3	9.5
B89	21.728	221.1166	C ₁₃ H ₁₇ O ₃	221.1172	-0.6	-2.8	5.5
B90	21.837	689.3893	C ₃₆ H ₅₈ O ₁₁ Na	689.3871	2.2	3.1	7.5
B91	21.963	429.1904	C ₂₄ H ₂₉ O ₇	429.1907	-0.4	-0.9	10.5
B92	22.235	689.3898	C ₃₆ H ₅₈ O ₁₁ Na	689.3871	2.7	3.9	7.5
B93 ^a	22.470	399.2174	C ₂₄ H ₃₁ O ₅	399.2166	0.8	2.0	9.5
B94	22.778	221.1167	C ₁₃ H ₁₇ O ₃	221.1172	-0.5	-2.4	5.5
B95	22.796	682.4173	C ₃₆ H ₆₀ NO ₁₁	682.4160	1.2	1.8	7.5
B96	22.940	221.1174	C ₁₃ H ₁₇ O ₃	221.1172	0.2	0.8	5.5
B97	23.393	381.2059	C ₂₄ H ₂₉ O ₄	381.2060	-0.1	-0.4	10.5
B98	23.465	381.2042	C ₂₄ H ₂₉ O ₄	381.2060	-1.8	-4.8	10.5
B99	23.592	381.2043	C ₂₄ H ₂₉ O ₄	381.2060	-1.7	-4.6	10.5
B100	23.664	381.2064	C ₂₄ H ₂₉ O ₄	381.2060	0.4	1.0	10.5

^a Unique metabolites only present in plasma.^a Common metabolites detected in bile and urine samples.

Table 3

Accurate mass measurements for the protonated molecules of metabolites in rat plasma (X).

No.	t_R (min)	Experimental m/z	Formula	Calculated m/z	mDa error	ppm error	DBE
X1	1.185	623.1606	C ₂₈ H ₃₁ O ₁₆	623.1606	-0.1	-0.1	13.5
X2	1.51	305.1236	C ₁₃ H ₂₁ O ₈	305.123	0.5	1.7	3.5
X3	2.831	451.1211	C ₂₁ H ₂₃ O ₁₁	451.1234	-2.4	-5.3	10.5
X4	2.849	479.19	C ₂₄ H ₃₁ O ₁₀	479.1911	-1.2	-2.5	9.5
X5	2.921	465.1394	C ₂₂ H ₂₅ O ₁₁	465.1391	0.3	0.6	10.5
X6	2.976	447.0927	C ₂₁ H ₁₉ O ₁₁	447.0921	0.5	1.1	12.5
X7	3.012	479.1902	C ₂₄ H ₃₁ O ₁₀	479.1911	-1.0	-2.0	9.5
X8	3.066	479.1566	C ₂₃ H ₂₇ O ₁₁	479.1547	1.8	3.8	10.5
X9	3.102	465.1727	C ₂₃ H ₂₉ O ₁₀	465.1755	-2.8	-6.1	9.5
X10	3.265	461.1056	C ₂₂ H ₂₁ O ₁₁	461.1078	-2.2	-4.9	12.5
X11	3.301	477.1017	C ₂₂ H ₂₁ O ₁₂	477.1027	-1.1	-2.2	12.5
X12	3.338	465.1392	C ₂₂ H ₂₅ O ₁₁	465.1391	0.1	0.1	10.5
X13	3.88	477.1049	C ₂₂ H ₂₁ O ₁₂	477.1027	2.1	4.5	12.5
X14	4.441	463.1234	C ₂₂ H ₂₃ O ₁₁	463.1234	-0.1	-0.2	11.5
X15	4.788	287.0575	C ₁₂ H ₁₅ O ₆ S	287.0583	-0.9	-3.1	5.5
X16	5.563	419.1318	C ₂₁ H ₂₃ O ₉	419.1336	-1.9	-4.4	10.5
X17	5.672	285.041	C ₁₂ H ₁₃ O ₆ S	285.0427	-1.7	-6.1	6.5
X18	5.69	451.1227	C ₂₁ H ₂₃ O ₁₁	451.1234	-0.8	-1.7	10.5
X19	5.798	477.1035	C ₂₂ H ₂₁ O ₁₂	477.1027	0.7	1.6	12.5
X20	5.798	419.132	C ₂₁ H ₂₃ O ₉	419.1336	-1.7	-4.0	10.5
X21	5.889	445.1103	C ₂₂ H ₂₁ O ₁₀	445.1129	-2.6	-5.9	12.5
X22	6.142	465.135	C ₂₂ H ₂₅ O ₁₁	465.1391	-4.1	-8.9	10.5
X23 ^a	6.196	463.1225	C ₂₂ H ₂₃ O ₁₁	463.1234	-1.0	-2.1	11.5
X24	6.269	355.0479	C ₁₅ H ₁₅ O ₈ S	355.0482	-0.3	-0.9	8.5
X25	6.323	509.1632	C ₂₄ H ₂₉ O ₁₂	509.1653	-2.2	-4.2	10.5
X26	6.377	493.1338	C ₂₃ H ₂₅ O ₁₂	493.134	-0.3	-0.5	11.5
X27	6.54	479.1552	C ₂₃ H ₂₇ O ₁₁	479.1547	0.4	0.9	10.5
X28	6.613	477.1386	C ₂₃ H ₂₅ O ₁₁	477.1391	-0.5	-1.1	11.5
X29	6.866	479.1537	C ₂₃ H ₂₇ O ₁₁	479.1547	-1.1	-2.3	10.5
X30	6.938	349.0364	C ₁₆ H ₁₃ O ₇ S	349.0376	-1.3	-3.6	10.5
X31 ^a	7.282	479.1193	C ₂₂ H ₂₃ O ₁₂	479.1184	0.9	1.9	11.5
X32	7.409	370.1303	C ₁₇ H ₂₄ NO ₆ S	370.1318	-1.6	-4.3	6.5
X33	9.182	352.1225	C ₁₇ H ₂₂ NO ₅ S	352.1213	1.2	3.3	7.5
X34 ^a	9.489	357.1319	C ₂₀ H ₂₁ O ₆	357.1332	-1.4	-3.8	10.5
X35 ^a	10.358	399.217	C ₂₄ H ₃₁ O ₅	399.2166	0.4	1.0	9.5
X36 ^a	12.674	513.3533	C ₃₀ H ₅₀ O ₅ Na	513.3561	-2.8	-5.5	5.5
X37 ^a	13.651	513.3535	C ₃₀ H ₅₀ O ₅ Na	513.355	-1.5	-3.0	5.5
X38 ^a	13.741	303.1085	C ₁₃ H ₁₉ O ₈	303.1074	1.1	3.5	4.5
X39	14.465	399.2133	C ₂₄ H ₃₁ O ₅	399.2166	-3.3	-8.3	9.5
X40 ^a	14.936	399.2139	C ₂₄ H ₃₁ O ₅	399.2166	-2.7	-6.8	9.5
X41 ^a	15.279	399.2139	C ₂₄ H ₃₁ O ₅	399.2166	-2.7	-6.8	9.5
X42 ^a	15.949	399.2163	C ₂₄ H ₃₁ O ₅	399.2166	-0.3	-0.8	9.5

^a Unique metabolites only present in plasma.

Table 4

Mass data for characterization of isoflavonoid-related metabolites only in rat bile (B).

No.	t_R (min)	Diagnostic molecular ions	Aglycone and other fragment ions	Origin	Major metabolic pathways
B41	7.054	[M+H] ⁺ 463.1245	[M-C ₆ H ₈ O ₆ +H] ⁺ 287.0921	Calycosin	Hydrogenation and glucuronidation
B46	7.326	[M+Na] ⁺ 485.1091 [M+NH ₄] ⁺ 480.1503	[M-CO ₂ -C ₆ H ₈ O ₆ +H] ⁺ 243.102		
B11	4.069	[M+H] ⁺ 435.1280	[M-C ₆ H ₈ O ₆ +H] ⁺ 259.0967	Calycosin, or formononetin, or HDMF	Demethylation, deoxygenation, hydrogenation and glucuronidation
B16	4.72	[M+NH ₄] ⁺ 452.1558			
B29	5.878	[M+Na] ⁺ 457.1087			
B32	6.204				
B37	6.692				
B45	7.253				
B15	4.575	[M+H] ⁺ 495.1482	[M-C ₆ H ₈ O ₆ +H] ⁺ 319.1175	DMP or HDMF	Hydration or hydroxylation and glucuronidation,
B22	5.353	[M+NH ₄] ⁺ 512.1754	[M-2H ₂ O+H] ⁺ 459.1272		
B24	5.57	[M+Na] ⁺ 517.13			
B51	7.778	[M+H] ⁺ 431.1369	[M-C ₆ H ₈ O ₆ +H] ⁺ 255.1051	Formononetin	Hydrogenation, dehydration and glucuronidation;
B83	14.545	[M+NH ₄] ⁺ 448.1646 [M+Na] ⁺ 453.12			
B65	10.04	[M+H] ⁺ 475.1258	[M-C ₆ H ₈ O ₆ +H] ⁺ 299.0934	DMP Calycosin or formononetin	Dehydrogenation and glucuronidation Hydroxylation, methylation and glucuronidation
B38	6.819	[M+H] ⁺ 491.1185 [M+Na] ⁺ 513.0981	[M-C ₆ H ₈ O ₆ +H] ⁺ 315.0893		
B14	4.503	[M+H] ⁺ 447.1277		Formononetin Calycosin-glc or formononetin-glc	Hydrogenation and glucuronidation Dihydroxylation
B3	3.254	[M+H] ⁺ 463.1252 [M+Na] ⁺ 485.1103 [M-H] ⁻ 461.0998	[M-C ₆ H ₁₀ O ₅ +H] ⁺ 301.0723		

Table 5

Mass data for characterization of phthalide-related metabolites only in rat bile.

No.	t_R (min)	Diagnostic molecular ions	Aglycone ion and other fragment ions	Origin	Major metabolic pathways
B61	9.099	[M+H] ⁺ 221.1167	[M-CH ₂ +H] ⁺ 207.1036	Butyridenepthalide	Hydration and methylation
B89	21.728	[M+Na] ⁺ 243.0966	[M-CH ₄ O+H] ⁺ 189.0906		
B94	22.778				
B96	22.94				
B97	23.393	[M+H] ⁺ 381.2059	191.1063	Ligustilide	Dimerization
B98	23.465	[M+NH ₄] ⁺ 398.2343			
B99	23.592	[M+Na] ⁺ 403.1879			
B100	23.664				
B40	6.982	[M+H] ⁺ 387.1648	[M-C ₆ H ₈ O ₆ +H] ⁺ 211.1297	Sendanenolide A	Hydration and glucuronidation
B55	8.375	[M+NH ₄] ⁺ 404.1919 [M+Na] ⁺ 409.1429	[M-C ₆ H ₈ O ₆ +H] ⁺ 211.133		
B74	11.306	[M+NH ₄] ⁺ 404.19 [M+Na] ⁺ 409.1458	[M-C ₆ H ₈ O ₆ +H] ⁺ 211.1315 [M-C ₆ H ₈ O ₆ -H ₂ O+H] ⁺ 193.12	Sendanenolide A	Hydration and glucuronidation
B47	7.344	[M+H] ⁺ 514.18	[M-C ₂ H ₅ NO ₂ +H] ⁺ 439.15		
B54	8.086		[M-C ₅ H ₇ NO ₃ +H] ⁺ 385.14 [M-C ₈ H ₁₁ N ₂ O ₆ +H] ⁺ 282.11 [M-C ₁₀ H ₁₇ O ₆ N ₃ S+H] ⁺ 207.10 189.09(C ₁₂ H ₁₃ O ₂) 161.10(C ₁₁ H ₁₃ O)	Ligustilide	Hydroxylation and glutathione conjugation
B44	7.163	[M+H] ⁺ 385.14	207.10 (C ₁₂ H ₁₅ O ₃)		
B48	7.525		189.09 (C ₁₂ H ₁₃ O ₂)		
B56	8.628		161.09 (C ₁₁ H ₁₃ O)		
B17	4.901	[M+H] ⁺ 368.1168	205.0855(C ₁₂ H ₁₃ O ₃)	Butyridenepthalide	glutathione conjugation and enzymatic hydrolysis
B21	5.191	[M+NH ₄] ⁺ 385.1436 [M+Na] ⁺ 390.0996	187.0746(C ₁₂ H ₁₁ O ₂) 171.0807(C ₁₂ H ₁₁ O)		

Table 6

Mass data for characterization of saponin-related metabolites in rat bile.

No.	t_R (min)	Diagnostic molecular ions	Characteristic fragment ions in positive ion mode
B86	19.883	[M+Na] ⁺ 675.4051(C ₃₆ H ₆₀ O ₁₀ Na) [M+HCOOH-H] ⁻ 697.4027(C ₃₇ H ₆₁ O ₁₂)	473.365(C ₃₀ H ₄₉ O ₄), 455.3503(C ₃₀ H ₄₇ O ₃), 437.3419(C ₃₀ H ₄₅ O ₂), 419.332(C ₃₀ H ₄₃ O), 143.1065(C ₈ H ₁₅ O ₂)
B87	20.281	[M+Na] ⁺ 645.3949(C ₃₅ H ₅₈ O ₉ Na) [2M+Na] ⁺ 1267.8053(C ₇₀ H ₁₁₆ O ₁₈ Na) [M+HCOOH-H] ⁻ 667.3925(C ₃₆ H ₅₉ O ₁₁)	[M-H ₂ O+H] ⁺ 605.4038, [M-2H ₂ O+H] ⁺ 587.3985, 473.3627(C ₃₀ H ₄₉ O ₄), 455.3499(C ₃₀ H ₄₇ O ₃), 437.3417(C ₃₀ H ₄₅ O ₂), 175.0602(C ₇ H ₁₁ O ₅), 143.1062(C ₈ H ₁₅ O ₂)
B90	21.819	[M+H] ⁺ 667.407(C ₃₆ H ₅₉ O ₁₁) [M+Na] ⁺ 689.3879(C ₃₆ H ₅₈ O ₁₁ Na) [M-H] ⁻ 665.3785(C ₃₆ H ₅₇ O ₁₁)	[M-H ₂ O+H] ⁺ 649.3918, [M-2H ₂ O+H] ⁺ 631.3839, 473.3622(C ₃₀ H ₄₉ O ₄), 455.3518(C ₃₀ H ₄₇ O ₃), 437.3405(C ₃₀ H ₄₅ O ₂), 419.3275(C ₃₀ H ₄₃ O), 143.1064(C ₈ H ₁₅ O ₂)
B92	22.235	[M+H] ⁺ 667.3913(C ₃₆ H ₅₉ O ₁₁) [M+Na] ⁺ 689.3894(C ₃₆ H ₅₈ O ₁₁ Na) [M-H] ⁻ 665.3765(C ₃₆ H ₅₇ O ₁₁)	[M-2H ₂ O+H] ⁺ 631.386, 455.3477(C ₃₀ H ₄₇ O ₃), 437.3404(C ₃₀ H ₄₅ O ₂), 419.3271(C ₃₀ H ₄₃ O), 143.1057(C ₈ H ₁₅ O ₂)
B95	22.796	[M+NH ₄] ⁺ 682.4173(C ₃₆ H ₆₀ NO ₁₁) [M+Na] ⁺ 687.3755(C ₃₆ H ₅₆ O ₁₁ Na) [M-H] ⁻ 663.3627(C ₃₆ H ₅₅ O ₁₁)	[M-C ₆ H ₈ O ₆ +H] ⁺ 489.3566, 471.3493(C ₃₀ H ₄₇ O ₄), 453.3424(C ₃₀ H ₄₅ O ₃), 409.3323(C ₂₅ H ₄₅ O ₄), 143.1052(C ₈ H ₁₅ O ₂)

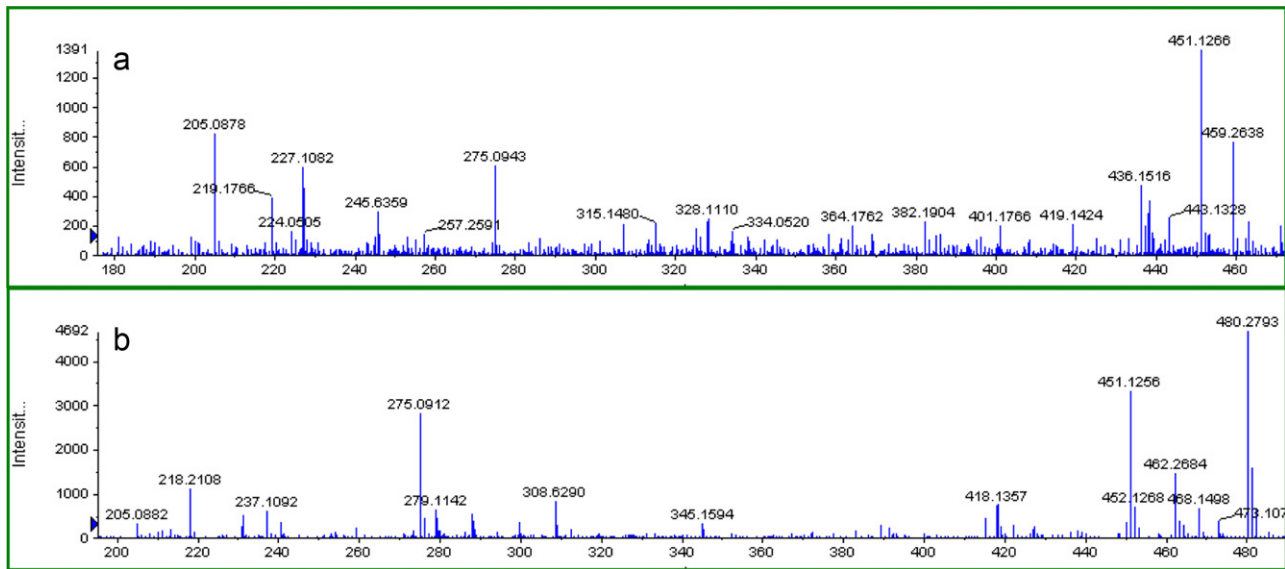


Fig. 3. TOFMS spectra of B13 (a) and B62 (b) with a fragmentor at 120 V in the positive ion mode.

Another group of isomers, B97, B98, B99 and B100, were considered as isomers of ligustilide dimer, which were consistent with the fact that phthalide dimer was present in both DBT preparation and the drug-containing urine [19,26]. B40, B55 and B74 were considered as

isomers of glucuronide conjugate according to the diagnostic loss of $C_6H_8O_6$. The aglycone was deduced to be hydration product of sen-danenolide A at the C6–7 double bond, as similar metabolic reaction was observed in the metabolism of ligustilide [27,28]. B17, B21,

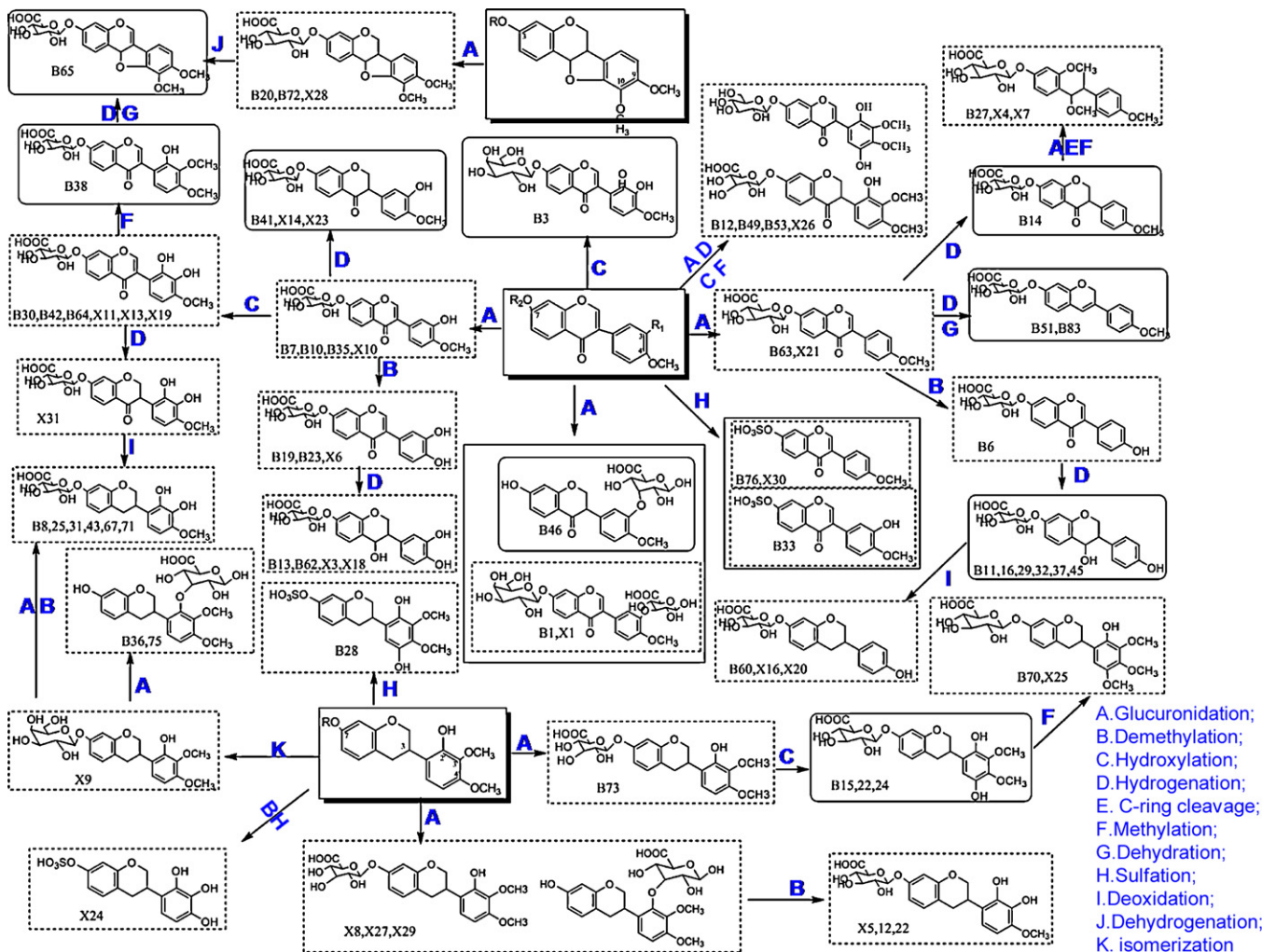


Fig. 4. Chemical structures of isoflavonoid-related metabolites in rat bile (B) and plasma (X) and the proposed major metabolic pathways of isoflavonoids.

B44, B48, B56, B47 and B54 were assigned as glutathione-derived compounds. As shown in Fig. 5, typical fragmentation patterns of glutathione conjugates [29] were observed in the mass spectra of B47 and B54, including diagnostic losses of 75 Da (glycine moiety, F1), 129 Da (*r*-glutamyl moiety, F2), and 307 Da (glutathione, F4). Therefore, B47 and B54 were identified as glutathione conjugates of monohydroxylated ligustilide, a pair of isomers that were also detected as metabolites of ligustilide [27]. Accordingly, B44, B48 and B56 were generated via loss of *r*-glutamyl moiety from B47 or B54. As for B17 and B21, diagnostic loss of C₅H₇NO₂S (145 Da) corresponding to the acetylcysteine residue, was observed in the process of formation of their common fragment ion at *m/z* 205.0838 (C₁₂H₁₃O₃). Similar to the identification of B78 [19], B17 and B21 were tentatively identified as acetylcysteine conjugate of monohydroxylated butylidenephthalide. In addition, despite lack of structure-related fragment ions, three metabolites B4, B5 and B9 were also simply assigned here as hydration products of B17 or B21, according to the elemental composition shift between them and the metabolism knowledge of ligustilide [27,28]. Based on the above structural analysis, chemical structures of phthalides metabolites in bile and metabolic pathways involved in their formation were summarized in Fig. 6.

3.2.1.3. Saponin-related metabolites. Five metabolites were detected from the drug-containing bile samples as metabolites of saponins. As shown in Table 6, the presence of the common fragment ions of DBT saponins at *m/z* 143.106, 419.331, 437.341, 455.352 and 473.362 in the positive ion mode indicated that B86, B87, B90 and B92 possessed the common 20,24-epoxy-9,19-cyclolanostane-3,6,16,25-tetrol skeleton (Fig. 7) as the aglycone [4]. The chemical formulas were ascertained as C₃₆H₆₀O₁₀ for B86, C₃₅H₅₈O₉ for B87, C₃₆H₅₈O₁₁ for B90 and C₃₆H₅₈O₁₁ for B92, by the presence of two or more molecular ions for each compound. The elemental shift from the molecular formula to the aglycone formula (C₃₀H₅₀O₅) suggested diagnostic losses for these four compounds including C₆H₁₀O₅ for B86, C₅H₈O₄ for B87, and C₆H₈O₆ for B90 and B92. As shown in Fig. 7, chemical analysis have demonstrated that most DBT saponins possessed the common sugar residues including xylose at the C3 position (R₁) and glucose at the C6 position (R₂) [4], so it was supposed that B86 and B87 were generated via hydrolysis at the C3 and C6 positions respectively. B90 and B92 were assigned as glucuronide conjugates of saponins aglycone while the conjugated positions remain unclear. B95 was also identified as glucuronide conjugate of saponins owing to the presence of diagnostic loss of C₆H₈O₆ and saponins-like characteristic fragment ions at *m/z* 489.3566 (aglycone ion), 471.3493, 453.3424 and 143.1052. All the former three fragment ions were 2 H less than the common fragment ions of DBT saponins, indicating this aglycone was formed via dehydrogenation of DBT saponins aglycone, while the last ion suggested that B95 possessed a intact 25-hydroxy-20,24-epoxy residue.

3.2.2. Characterization of metabolites in plasma

In plasma sample pretreatment, SPE alone cannot totally remove protein from plasma, especially for small molecule protein. Consequently, we conducted protein precipitation before running SPE. As shown in Table 3, a total of forty two compounds were detected as metabolites of DBT from the drug-containing plasma samples, including ten unique metabolites only present in plasma and thirty two metabolites also found in urine and/or bile. The mass data for characterization of these metabolites was summarized in Table 7. As for the ten unique metabolites, X35, X40, X41 and X42 were considered as isomers of X39 owing to the common molecular ions and/or fragment ions, while X23 was assigned as isomer of X14. The presence of X34 and X38 was proved by the coexistence of

their protonated and deprotonated ions in relatively high abundance in plasma. But no diagnostic fragment ions were obtained for their structural elucidation. Diagnostic loss of C₆H₈O₆ demonstrated that X31 was a glucuronide conjugate, and the aglycone was one water molecule more than calycosin, indicating that it may be generated via hydroxylation and hydrogenation of calycosin [21]. X36 and X37 were assigned as isomers of saponins due to the presence of common [M+Na]⁺ at *m/z* 513.35 and common diagnostic ions of DBT saponins at *m/z* 473.36, 455.35, 437.34 and 143.107. Since hydrolysis of the ether glycosidic bonds was a common metabolic pathway of saponins, X36 and X37 were assigned as aglycones of DBT saponins. In summary, twenty eight were tentatively assigned as metabolites of isoflavonoids in plasma (Fig. 4), ten were referred as metabolites of phthalides (Fig. 6), and two were identified as metabolites of saponins (Fig. 7).

3.3. Correlative analysis of metabolite profiling in rat biological fluids

The metabolites characterized in this work provided a global view of qualitative metabolite profiles of DBT in rat bile and plasma, which enriched and also partly validated the results of the previous study on rat urinary metabolite profile [19]. Comparing with the rat urinary metabolite profile of DBT, rat bile contained much more complex forms of metabolites. The metabolite profile in plasma showed us the main circulating forms of DBT, which were more closely related to the bioactivity. Similar to the previous study on rat urine [19], all three kinds of major constituents, isoflavonoids, phthalides and saponins, were detected as both parent compounds and metabolites in bile and plasma, further demonstrating that they should serve as bioactive components of DBT. It should be noted that in comparison with urine and plasma, rat bile appears to contain relatively more glutathione-derived and saponin-related compounds but fewer sulfate conjugates. This phenomenon may result from the fact that the former two types of constituents possessed higher molecular mass.

Similar to urine analysis, isoflavonoids were the most prevalent drug-related compounds in bile and plasma. A total of eight parent compounds and fifty metabolites were detected and tentatively identified as isoflavonoids in bile, and about half of them were not detected in rat urine. Meanwhile, five parent compounds and twenty eight metabolites in plasma were isoflavonoid-related compounds. The presence of various isoflavonoid-related metabolites in urine, bile and plasma indicated that isoflavonoids of DBT were subjected into extensive *in vivo* metabolism. As shown in Fig. 4, typical drug metabolic reactions were involved in the formation of these metabolites, containing phase I reactions, such as demethylation, hydroxylation, hydrogenation, methylation, dehydration, deoxidation and dehydrogenation, and phase II reactions such as glucuronidation and sulfation. The presence of M16 and M18 in urine [19], B27 in bile, and X4 and X7 in plasma indicated that C-ring cleavage was also a metabolic pathway of DBT isoflavonoids. It was presumed that these C-ring cleavage metabolites were generated via intestinal bacteria and then absorbed into blood [24]. In addition, the identification of metabolites B1 (X1), B3 and X9, as well as the detection of parent compounds Pp1, Pb4 (Pp3), Pb5, Pb6 (Pp4) and Pb7-9, further proved that isoflavonoid glycosides can be directly absorbed into the circulating system [19,30,31].

As for phthalides, rat bile contained four parent compounds, Z-ligustilide and three isomers of senkyunolide, while rat plasma contained only one senkyunolide. Biliary metabolites of phthalides were more diverse than urine. Up to forty compounds in bile and ten compounds in plasma were assigned as phthalide-related metabolites, and almost all metabolites in urine and plasma were present in bile. As shown in Fig. 6, various metabolic reactions

Table 7

Mass data for characterization of metabolites in rat plasma.

No.	t_R (min)	Diagnostic molecular ions	Fragment ions	Origin	Major metabolic pathways	Other sources
X1	1.185	[M+H] ⁺ 623.1606 [M+Na] ⁺ 645.1434	461.1088, 285.074	Calycosin-glc	Glucuronidation	Urine and bile
X2	1.51	[M+H] ⁺ 305.1236		Phthalides	Hydration and/or hydroxylation, methylation	Urine and bile
X3	2.831	[M+H] ⁺ 451.1211 [M+NH ₄] ⁺ 468.1497 [M+Na] ⁺ 473.1081 [M+H] ⁺ 479.19	275.0904, 139.0411, 123.0438	Calycosin, formononetin, or HDMF	Demethylation, hydrogenation and/or hydroxylation and glucuronidation	Urine and bile
X4	2.849	[M+Na] ⁺ 501.1762 [M+H] ⁺ 479.19	285.151	Formononetin	C-ring cleavage, methylation and glucuronidation	Urine
X5	2.921	[M+H] ⁺ 465.1394	289.1042	HDMF	Demethylation, and glucuronidation	Urine and bile
X6	2.976	[M+H] ⁺ 447.0927 [M+Na] ⁺ 445.0717		Calycosin	Demethylation, and glucuronidation	Urine and bile
X7	3.012	[M+H] ⁺ 479.1902 [M+Na] ⁺ 501.1814	285.1495	Formononetin	C-ring cleavage, methylation and glucuronidation	Urine and bile
X8	3.084	[M+H] ⁺ 479.1566	303.1233, 167.0702, 133.0647, 123.044	HDMF	Glucuronidation	Bile
X9	3.102	[M+H] ⁺ 465.1727 [M+Na] ⁺ 487.1545	303.1227, 167.0702, 123.0454	Glucoside of HDMF	Isomerization	Urine and bile
X10	3.265	[M+H] ⁺ 461.1056	285.0768	Calycosin	Glucuronidation	Urine and bile
X11	3.301	[M+H] ⁺ 477.1017	301.0707, 285.0715, 123.0423	Calycosin or formononeti	Hydroxylation and glucuronidation	bile
X12	3.338	[M+H] ⁺ 465.1388 [M+NH ₄] ⁺ 482.1668	289.1069	HDMF	Demethylation, and glucuronidation	Urine and bile
X13	3.88	[M+H] ⁺ 477.1049	301.0712, 285.0708, 123.0422	Calycosin or formononetin	Hydroxylation and glucuronidation	Urine and bile
X14	4.441	[M+H] ⁺ 463.1234 [M+NH ₄] ⁺ 480.152	287.0907, 153.0553, 135.0428	Calycosin	Hydrogenation and glucuronidation	Bile
X15	4.788	[M+H] ⁺ 287.0575		Butylidenephthalide	Hydration and sulfation	Urine
X16	5.563	[M+H] ⁺ 419.1318 [M+NH ₄] ⁺ 436.1563 [M+Na] ⁺ 441.1154	383.1132, 243.0999, 133.0647, 123.0444	Formononetin	Demethylation, hydrogenation, deoxidation and glucuronidation	Urine and bile
X17	5.672	[M+H] ⁺ 285.041		Butylidenephthalide	Hydroxylation and sulfation	Urine and bile
X18	5.69	[M+H] ⁺ 451.1227 [M+NH ₄] ⁺ 468.1491 [M+Na] ⁺ 473.1068	275.0908, 167.0632, 165.0548, 139.0391, 123.0457, 121.0299	Calycosin, formononetin, or HDMF	Demethylation, hydrogenation and/or hydroxylation and glucuronidation	Urine and bile
X19	5.798	[M+H] ⁺ 477.1035	301.0696, 167.0659, 133.0643, 123.0453	Calycosin or formononetin	Hydroxylation and glucuronidation	Urine and bile
X20	5.798	[M+H] ⁺ 419.132 [M+NH ₄] ⁺ 436.1596 [M+Na] ⁺ 441.1148	383.1112, 243.0995	Formononetin	Demethylation, hydrogenation, deoxidation and glucuronidation	Urine
X21	5.889	[M+H] ⁺ 445.1103	269.0803, 254.0575	Formononetin	Glucuronidation	Urine and bile
X22	6.142	[M+H] ⁺ 465.135 [M+NH ₄] ⁺ 482.1657 [M-H] ⁻ 463.1189 [M+Na] ⁺ 487.1198	289.1041	HDMF	Demethylation, and glucuronidation	Urine and bile
X23	6.196	[M+H] ⁺ 463.1225 [M+Na] ⁺ 485.1303	287.0915, 177.0599	Calycosin	Hydrogenation and glucuronidation	ND

Table 7 (Continued)

No.	t _R (min)	Diagnostic molecular ions	Fragment ions	Origin	Major metabolic pathways	Other sources
X24	6.269	[M+H] ⁺ 355.0479		HDMF	Demethylation and sulfation	Urine
X25	6.323	[M+H] ⁺ 509.1632 [M+NH ₄] ⁺ 526.1875	333.1313	HDMF	Hydroxylation, methylation and glucuronidation	Urine and bile
X26	6.377	[M+H] ⁺ 493.1338 [M+NH ₄] ⁺ 510.155 [M+Na] ⁺ 515.11	317.1015	Calycosin or formononetin	Methylation, hydrogenation, hydroxylation and glucuronidation	Urine and bile
X27	6.54	[M+H] ⁺ 479.1552 [M+NH ₄] ⁺ 496.1806 [M+Na] ⁺ 501.1347	461.1405, 443.1322, 303.1212, 167.0698, 123.0438	HDMF	Glucuronidation	Urine and bile
X28	6.613	[M+H] ⁺ 477.1386 [M+NH ₄] ⁺ 494.1653 [M+Na] ⁺ 499.1202	301.1069, 167.0703, 152.0468, 123.0451	DMP	Glucuronidation	Urine and bile
X29	6.866	[M+H] ⁺ 479.1537 [M+NH ₄] ⁺ 496.1783 [M+Na] ⁺ 501.1282	303.1219, 167.0698, 123.0437	HDMF	Glucuronidation	Urine and bile
X30	6.938	[M+H] ⁺ 349.0364		Formononetin	Sulfation	Urine and bile
X31	7.282	[M+H] ⁺ 479.1193 [M+NH ₄] ⁺ 496.145	447.1269, 303.0835	Calycosin or formononetin	Hydrogenation, hydroxylation and glucuronidation	ND
X32	7.409	[M+H] ⁺ 370.1303 [M+Na] ⁺ 392.1124	237.1107, 221.0806, 205.0833	Phthalides	Oxidation, glutathione conjugation, enzymatic hydrolysis	Urine and bile
X33	9.182	[M+H] ⁺ 352.1225		Phthalides	Oxidation, glutathione conjugation, enzymatic hydrolysis	Urine and bile
X34	9.489	[M+H] ⁺ 357.1319		Not identified		ND
X35	10.358	[M+H] ⁺ 399.217		Liguistilide	Dimerization and hydration	ND
X36	12.674	[M+Na] ⁺ 513.3533	473.3607, 455.3522, 437.3351,	Saponins	Hydrolysis	ND
X37	13.651	[M+Na] ⁺ 513.3535	143.1066			ND
X38	13.741	[M+H] ⁺ 303.1085		Not identified		ND
X39	14.465	[M+H] ⁺ 399.2133	381.2042, 191.1048	Liguistilide	Dimerization and hydration	Urine and bile
X40	14.936	[M+Na] ⁺ 421.2012				ND
X41	15.279					ND
X42	15.949					ND

ND: not detected.

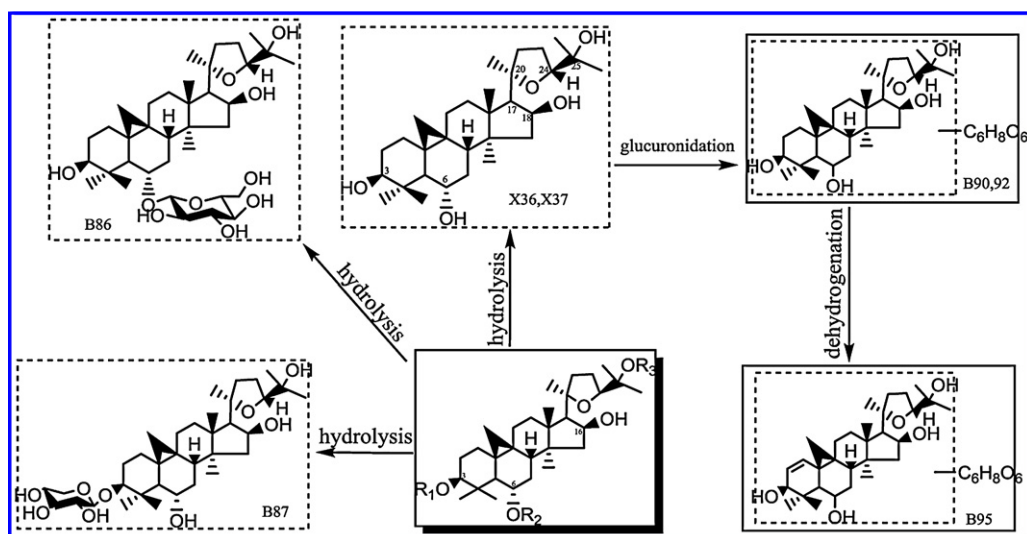


Fig. 7. Chemical structures of saponin-related metabolites in rat bile (B) and plasma (X) and the proposed major metabolic pathways of saponins.

such as dimerization, hydration, hydroxylation, glucuronidation, sulfation, glutathione conjugation and sequential hydrolysis and acetylation were involved in the metabolism of phthalides. Unlike isoflavonoids, glucuronide conjugates of phthalides were present in urine and bile, but absent in plasma.

Previous study suggested that only very low amounts of astragaloside IV and astragaloside V/VI/VII were present in rat urine. However, as shown in Fig. 7, DBT saponins were detected and characterized as various parent forms and metabolites in rat bile and plasma with relatively high amount, which partly validated our previous speculations [19]. Four saponins were detected from the drug-containing plasma, indicating that parent compounds such as astragaloside IV, astragaloside V/VI/VII and saponins aglycones were the main circulating forms of DBT saponins. Whether they were directly absorbed into blood or indirectly absorbed after hydrolysis via intestinal bacteria was still unclear. In bile, seven parent compounds and five metabolites were assigned as saponins, indicating that biliary excretion may be the main route for clearance of DBT saponins. The identification of five saponin metabolites suggested that typical phase II reactions such as glucuronidation could facilitate the excretion of saponins via bile. As shown in Fig. 7, hydrolysis, glucuronidation and dehydrogenation were considered to be three major metabolic pathways of DBT saponins.

The content of metabolites in plasma was generally much higher than that of parent compounds based on comparison of their peak heights in EICs, indicating that the absorbed components of DBT may be mainly present in the blood as different forms of metabolites. The fact that DBT possessed various biological effects suggested that these metabolites may retain some biological activities. According to the rank of the peak heights, X28, X21 and X27, corresponding to glucuronide conjugates of DMP, formononetin and HDMF respectively, were considered as the three major isoflavonoid-related compounds in plasma, indicating that glucuronidation was the most predominant metabolic pathway of isoflavonoids in circulating system. A group of isomers (X39, X41 and X42), X32 as well as Pp2 (senkyunolide) were the main circulating phthalide-related metabolites, suggesting that dimmers, acetylcysteine conjugates and parent compound were the major forms of phthalides in plasma. Saponins were present in plasma predominantly as aglycone forms (X36 and X37), and accordingly, hydrolysis was considered to be major metabolic pathway of saponins in circulating system.

4. Conclusion

In this work, the metabolite profiles of DBT in rat bile and plasma were qualitatively described by RRLC–TOFMS method, and the possible metabolic pathways of DBT were subsequently proposed. The characterization of biliary metabolites suggested that rat bile contained much more DBT-related metabolites than urine, indicating that after oral administration, DBT was subjected into extensive *in vivo* metabolism to facilitate its excretion from body. The parent compounds and metabolites identified in plasma suggested the main circulating forms of DBT, which may be directly related to its therapeutic effect. Further investigation was required to elucidate the pharmacokinetic properties of these major DBT-related plasma compounds and clarify their pharmacological activity. Besides, this study further demonstrated the effectiveness of the RRLC–TOFMS approach in the *in vivo* metabolism field of Chinese herbal medicines.

Acknowledgement

Contract/grant sponsor: the National Science and Technology Major Project 'Creation of Major New Drugs' from China, and Program for Changjiang Scholars and Innovative Research Team in University; contract/grant number: 2009ZX09502-020 and IRT0868.

References

- [1] Q.T. Gao, J.K. Cheung, R.C. Choi, W.W. Cheung, J. Li, Z.Y. Jiang, R. Duan, K.J. Zhao, A.W. Ding, T.T. Dong, K.W. Tsim, A chinese herbal decoction prepared from Radix Astragali and Radix Angelicae Sinensis induces the expression of erythropoietin in cultured Hep3B cells, *Planta Med.* 74 (2008) 392–395.
- [2] Q.T. Gao, J. Li, J.K. Cheung, J. Duan, A.W. Ding, A.W. Cheung, K.J. Zhao, W.Z. Li, T.T. Dong, K.W. Tsim, Verification of the formulation and efficacy of Danggui Buxue Tang (a decoction of Radix Astragali and Radix Angelicae Sinensis): an exemplifying systematic approach to revealing the complexity of chinese herbal medicine formulae, *Chin. Med.* 2 (2007) 12–22.
- [3] L. Yi, L.W. Qi, P. Li, Y.H. Ma, Y.J. Luo, H.Y. Li, Simultaneous determination of bioactive constituents in Danggui Buxue Tang for quality control by HPLC coupled with a diode array detector, an evaporative light scattering detector and mass spectrometry, *Anal. Bioanal. Chem.* 389 (2007) 571–580.
- [4] L.W. Qi, X.D. Wen, J. Cao, C.Y. Li, P. Li, L. Yi, Y.X. Wang, X.L. Cheng, X.X. Ge, Rapid and sensitive screening and characterization of phenolic acids, phthalides, saponins and isoflavonoids in Danggui Buxue Tang by rapid resolution liquid chromatography/diode-array detection coupled with time-of-flight mass spectrometry, *Rapid Commun. Mass Spectrom.* 22 (2008) 2493–2509.
- [5] L.W. Qi, J. Cao, P. Li, Y.X. Wang, Rapid and sensitive quantitation of major constituents in Danggui Buxue Tang by ultra-fast HPLC–TOF/MS, *J. Pharm. Biomed. Anal.* 49 (2009) 502–507.

- [6] X. Zhang, L.W. Qi, L. Yi, P. Li, X.D. Wen, Q.T. Yu, Screening and identification of potential bioactive components in a combined prescription of Danggui Buxue decoction using cell extraction coupled with high performance liquid chromatography, *Biomed. Chromatogr.* 22 (2008) 157–163.
- [7] S.L. Li, P. Li, L.H. Sheng, R.Y. Li, L.W. Qi, L.Y. Zhang, Live cell extraction and HPLC–MS analysis for predicting bioactive components of traditional chinese medicines, *J. Pharm. Biomed. Anal.* 41 (2006) 576–581.
- [8] X.D. Wen, L.W. Qi, J. Chen, Y. Song, L. Yi, X.W. Yang, P. Li, Analysis of interaction property of bioactive components in Danggui Buxue Decoction with protein by microdialysis coupled with HPLC–DAD–MS, *J. Chromatogr. B* 852 (2007) 598–604.
- [9] L.H. Sheng, S.L. Li, L. Kong, X.G. Chen, X.Q. Mao, X.Y. Su, H.F. Zou, P. Li, Separation of compounds interacting with liposome membrane in combined prescription of traditional chinese medicines with immobilized liposome chromatography, *J. Pharm. Biomed. Anal.* 38 (2005) 216–224.
- [10] L.W. Qi, P. Li, S.L. Li, L.H. Sheng, R.Y. Li, Y. Song, H.J. Li, Screening and identification of permeable components in a combined prescription of Danggui Buxue decoction using a liposome equilibrium dialysis system followed by HPLC and LC–MS, *J. Sep. Sci.* 29 (2006) 2211–2220.
- [11] C. Chen, F.J. Gonzalez, J.R. Idle, LC–MS–based metabolomics in drug metabolism, *Drug Metab. Rev.* 39 (2007) 581–597.
- [12] X.D. Wen, L.W. Qi, P. Li, K.D. Bao, X.W. Yan, L. Yi, C.Y. Li, Simultaneous determination of calycosin-7-O-beta-D-glucoside, ononin, astragaloside IV, astragaloside I and ferulic acid in rat plasma after oral administration of Danggui Buxue Tang extract for their pharmacokinetic studies by liquid chromatography–mass spectrometry, *J. Chromatogr. B* 865 (2008) 99–105.
- [13] P. Wang, Y. Liang, N. Zhou, B. Chen, L. Yi, Y. Yu, Z. Yi, Screening and analysis of the multiple absorbed bioactive components and metabolites of Danggui Buxue decoction by the metabolic fingerprinting technique and liquid chromatography/diode-array detection mass spectrometry, *Rapid Commun. Mass Spectrom.* 21 (2007) 99–106.
- [14] D.F. Toh, L.S. New, H.L. Koh, E.C. Chan, Ultra-high performance liquid chromatography/time-of-flight mass spectrometry (UHPLC/TOFMS) for time-dependent profiling of raw and steamed panax notoginseng, *J. Pharm. Biomed. Anal.* 52 (2010) 43–50.
- [15] G. Xie, R. Plumb, M. Su, Z. Xu, A. Zhao, M. Qiu, X. Long, Z. Liu, W. Jia, Ultra-performance LC/TOF MS analysis of medicinal panax herbs for metabolomic research, *J. Sep. Sci.* 31 (2008) 1015–1026.
- [16] N. Zhang, S.T. Fountain, H. Bi, D.T. Rossi, Quantification and rapid metabolite identification in drug discovery using API time-of-flight LC/MS, *Anal. Chem.* 72 (2000) 800–806.
- [17] R.J. Mortishire-Smith, D. O'Connor, J.M. Castro-Perez, J. Kirby, Accelerated throughput metabolic route screening in early drug discovery using high-resolution liquid chromatography/quadrupole time-of-flight mass spectrometry and automated data analysis, *Rapid Commun. Mass Spectrom.* 19 (2005) 2659–2670.
- [18] M. Wrona, T. Mauriala, K.P. Bateman, R.J. Mortishire-Smith, D. O'Connor, 'All-in-one' analysis for metabolite identification using liquid chromatography/hybrid quadrupole time-of-flight mass spectrometry with collision energy switching, *Rapid Commun. Mass Spectrom.* 19 (2005) 2597–2602.
- [19] C.Y. Li, L.W. Qi, P. Li, X.D. Wen, Y.F. Zhu, E.H. Liu, Z. Gong, X.L. Yang, M.T. Ren, Y.J. Li, X.X. Ge, Identification of metabolites of Danggui Buxue Tang in rat urine by liquid chromatography coupled with electrospray ionization time-of-flight mass spectrometry, *Rapid Commun. Mass Spectrom.* 23 (2009) 1977–1988.
- [20] T. Kind, O. Fiehn, Seven Golden Rules for heuristic filtering of molecular formulas obtained by accurate mass spectrometry, *BMC Bioinformatics* 8 (2007) 105–125.
- [21] S.M. Heinonen, A. Hoikkala, K. Wahala, H. Adlercreutz, Metabolism of the soy isoflavones daidzein, genistein and glycitein in human subjects. Identification of new metabolites having an intact isoflavonoid skeleton, *J. Steroid Biochem. Mol. Biol.* 87 (2003) 285–299.
- [22] D.B. Clarke, A.S. Lloyd, N.P. Botting, M.F. Oldfield, P.W. Needs, H. Wiseman, Measurement of intact sulfate and glucuronide phytoestrogen conjugates in human urine using isotope dilution liquid chromatography–tandem mass spectrometry with [¹³C(3)]isoflavone internal standards, *Anal. Biochem.* 309 (2002) 158–172.
- [23] J. Bursztyka, E. Perdu, J. Tulliez, L. Debrauwer, G. Delouis, C. Canlet, G. De Sousa, R. Rahmani, E. Benfenati, J.P. Cravedi, Comparison of genistein metabolism in rats and humans using liver microsomes and hepatocytes, *Food Chem. Toxicol.* 46 (2008) 939–948.
- [24] C.S. Hwang, H.S. Kwak, H.J. Lim, S.H. Lee, Y.S. Kang, T.B. Choe, H.G. Hur, K.O. Han, Isoflavone metabolites and their in vitro dual functions: they can act as an estrogenic agonist or antagonist depending on the estrogen concentration, *J. Steroid Biochem. Mol. Biol.* 101 (2006) 246–253.
- [25] S. Heinonen, K. Wahala, H. Adlercreutz, Identification of isoflavone metabolites dihydrodaidzein, dihydrogenistein, 6'-OH-O-dma, and cis-4-OH-equol in human urine by gas chromatography–mass spectroscopy using authentic reference compounds, *Anal. Biochem.* 274 (1999) 211–219.
- [26] L. Yi, Y. Liang, H. Wu, D. Yuan, The analysis of Radix Angelicae Sinensis (Danggui), *J. Chromatogr. A* 1216 (2009) 1991–2001.
- [27] R. Yan, N.L. Ko, S.L. Li, Y.K. Tam, G. Lin, Pharmacokinetics and metabolism of ligustilide, a major bioactive component in Rhizoma Chuanxiong, in the rat, *Drug Metab. Dispos.* 36 (2008) 400–408.
- [28] C. Ding, Y. Sheng, Y. Zhang, J. Zhang, G. Du, Identification and comparison of metabolites after oral administration of essential oil of Ligusticum chuanxiong or its major constituent ligustilide in rats, *Planta Med.* 74 (2008) 1684–1692.
- [29] B.M. Johnson, A.V. Kamath, J.E. Leet, X. Liu, R.S. Bhide, R.W. Tejwani, Y. Zhang, L. Qian, D.D. Wei, L.J. Lombardo, Y.Z. Shu, Metabolism of 5-isopropyl-6-(5-methyl-1,3,4-oxadiazol-2-yl)-N-(2-methyl-1H-pyrrolo[2,3-b]pyridin-5-yl)pyrrolo[2,1-f][1,2,4]triazin-4-amine (BMS-645737): identification of an unusual N-acetylglucosamine conjugate in the cynomolgus monkey, *Drug Metab. Dispos.* 36 (2008) 2475–2483.
- [30] F. Xu, Y. Zhang, S. Xiao, X. Lu, D. Yang, X. Yang, C. Li, M. Shang, P. Tu, S. Cai, Absorption and metabolism of Astragali radix decoction: in silico, in vitro, and a case study in vivo, *Drug Metab. Dispos.* 34 (2006) 913–924.
- [31] L. Zhang, Z. Zuo, G. Lin, Intestinal and hepatic glucuronidation of flavonoids, *Mol. Pharmacol.* 4 (2007) 833–845.